

pubs.acs.org/JACS Article

Controlling Molecular Photoisomerization in Photonic Cavities through Polariton Funneling

Inki Lee, Sarah R. Melton, Ding Xu, and Milan Delor*



Metallic mirror

Polariton funneling enables isomer-selective isomerization

Metallic mirror

Selective photoisomerization

Selective photoisomerization

Selective photoisomerization

Selective photoisomerization

ABSTRACT: Strong coupling between photonic modes and molecular electronic excitations, creating hybrid light-matter states called polaritons, is an attractive avenue for controlling chemical reactions. Nevertheless, experimental demonstrations of polariton-modified chemical reactions remain sparse. Here, we demonstrate modified photoisomerization kinetics of merocyanine and diarylethene by coupling the reactant's optical transition with photonic microcavity modes. We leverage broadband Fourier-plane optical microscopy to noninvasively and rapidly monitor photoisomerization within microcavities, enabling systematic investigation of chemical kinetics for different cavity-exciton detunings and photoexcitation conditions. We demonstrate three distinct effects of cavity coupling: first, a renormalization of the photonic density of states, akin to a Purcell effect, leads to enhanced absorption and isomerization rates at certain wavelengths, notably red-shifting the onset of photoisomerization. This effect is present under both strong and weak light-matter couplings. Second, kinetic competition between polariton localization into reactive molecular states and cavity losses leads to a suppression of the photoisomerization yield. Finally, our key result is that in reaction mixtures with multiple reactant isomers, exhibiting partially overlapping optical transitions and distinct isomerization pathways, the cavity resonance can be tuned to funnel photoexcitations into specific reactant isomers. Thus, upon decoherence, polaritons localize into a chosen isomer, selectively triggering the latter's photoisomerization despite initially being delocalized across all isomers. This result suggests that careful tuning of the cavity resonance is a promising avenue to steer chemical reactions and enhance product selectivity in reaction mixtures.

■ INTRODUCTION

Strong coupling between light and polar excitations (including excitons and vibrations) can renormalize light-matter eigenstates into part-light part-matter states known as polaritons. ^{1,2} Polaritonic strong coupling is typically achieved in the collective regime, whereby many dipoles collectively couple to the same photonic mode, such as in an optical microcavity. ^{3–8} Polaritons inherit the dispersive nature of photonic modes and are delocalized in space but maintain relatively strong matter-like interactions. These features have been leveraged to enhance energy transport, ^{9–15} realize Bose–Einstein condensation, ^{16–18} and achieve single-photon nonlinearities. ^{19–23} Strong light-matter coupling is also an emerging route to control chemical reactions. ^{4–6,24–27} In this context, vibrational strong coupling has been more heavily explored both experimentally ^{28–32} and theoretically. ^{33–38} Here

we focus on electronic strong coupling, wherein the electronic transitions of reactant molecules are hybridized with microcavity photons. 14,39,40,42 Specifically, we study how the photoisomerization rates of two organic photoswitches are modified in microcavities.

Some theoretical work predicts large effects of electronic strong coupling on photochemistry, including modifications of potential energy surfaces along which reactions evolve. 33,43–49

Received: October 11, 2023
Revised: February 26, 2024
Accepted: March 7, 2024
Published: March 26, 2024

Metallic mirror





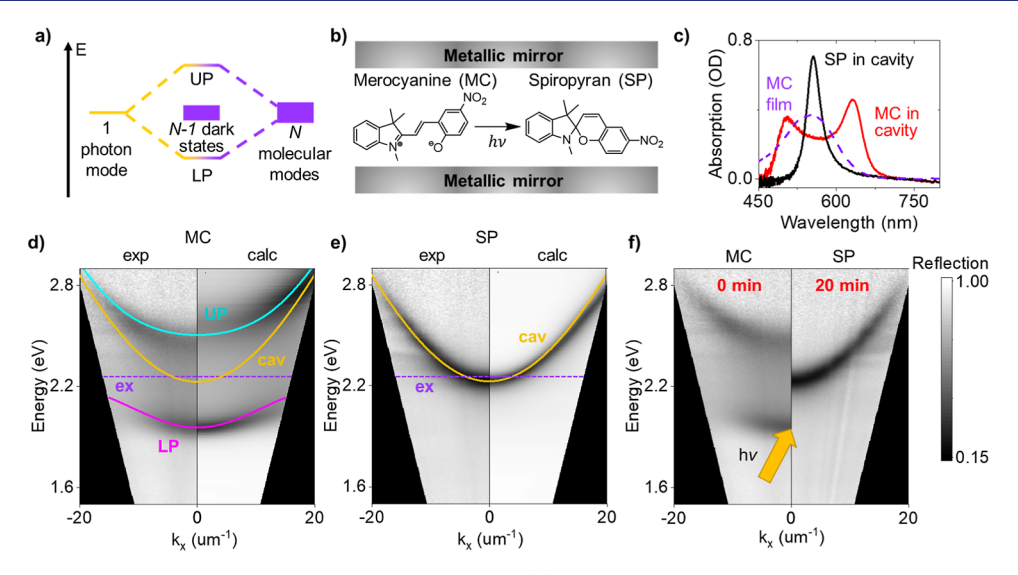


Figure 1. Tracking photoisomerization under strong light-matter coupling. (a) Tavis—Cummings model for collective strong coupling. (b) Sample configuration of MC photoisomerization in an optical microcavity. MC is dispersed in PMMA to control the cavity thickness. (c) Visible absorption spectra of SP and MC placed in a microcavity (black and red, respectively) and MC outside the cavity (purple). The SP form, which does not absorb visible light, displays primarily a bare photonic cavity mode. In MC form, the photonic mode splits into the upper and lower polaritons. (d,e) Experimental (left) and transfer matrix calculations (right) broadband angle-resolved reflectance of strongly coupled MC (d) and SP (e) in silver microcavities. Colored lines overlaid on the dispersion are fits using a COM. The purple dashed lines indicate the peaks of the MC exciton transition. (f) Experimental angle-resolved spectra during a photoisomerization experiment. The arrow represents the excitation wavelength and momentum.

Despite these advances, and multiple experimental demonstrations of energy-level tuning and rate inversions in molecular systems, ^{39,50-54} there are few experimental demonstrations of polariton-driven chemical transformations in the electronic strong-coupling regime. A pioneering study by Ebbesen and co-workers⁴² showed that the rate of the ringopening photoisomerization of spiropyran (SP) into merocyanine (MC) was slowed by approximately an order of magnitude in cavities that were tuned to be resonant with the product state. 42 Recent studies reproduce this empirical finding, 55,56 though one study suggests that the effect is nonpolaritonic. 56 In this work, we study the opposite reaction from MC to SP, with the reactant (rather than the product) strongly coupled to the cavity mode. A recent study by Börjesson and co-workers⁴¹ studied the effect of electronic strong coupling on a norbornadiene-quadricyclane photoswitch with the reactant state of the photoswitch strongly coupled to the cavity. Although this study shows a suppression of the photoisomerization yield, strong coupling enables lowering of the photon energy required to drive photoisomerization. Finally, recent work by Stern and co-workers⁵⁵ shows that the photoswitching kinetics of fulgides is accelerated by cavity strong coupling.

Questions remain about why polaritons influence chemical reactions. In the Tavis—Cummings model of collective strong-coupling, N molecules couple to one cavity mode, resulting in two bright states—known as the upper polariton (UP) and lower polariton (LP)—and N-1 dark states that are also collective in nature but formally do not couple to the light field except in the presence of disorder (Figure 1a). Given that N is often on the order of 10^5 to 10^6 , dark states outweigh bright states 49,57,58 and dominate system relaxation with dynamics resembling those of bare molecules, $^{49,59-63}$ raising questions on why cavities affect chemical reactions. Although proposals suggest that dark states can inherit some delocalized character that can modify reactions, 35,64,65 another possibility is that

cavity-induced effects on light-driven reactions stem primarily from a (weak-coupling) Purcell effect that is not intrinsically polaritonic. 56,66,67 Although not explored in the context of chemical reactions, other proposals suggest that when cavity modes are resonant with product states, polaritons can funnel energy toward these states and change photophysical pathways, even if the density of dark states far outweighs polaritons. 45,68-70 Here, through systematic investigations of photoisomerization rates using different cavity-exciton detunings, photoexcitation wavelengths, and light-matter coupling regimes, we show that both Purcell-like effects and polariton funneling are operative mechanisms that enable tuning the absorption onset, relaxation dynamics, and most importantly chemical reaction pathways in organic microcavities.

■ RESULTS AND DISCUSSION

Tracking Photoisomerization Kinetics with Broadband Fourier-Plane Microscopy. The reactant molecules chosen for this study are the colored MC form of the SP derivative 1',3'-dihydro-1',3',3'-trimethyl-6-nitrospiro[2*H*-1benzopyran-2,2'-(2H)-indole], Figure 1b, and the colored closed ring isomer of the diarylethene (DAE) derivative 1,2bis(2,4-dimethyl-5-phenyl-3-thienyl)-3,3,4,4,5,5-hexafluoro-1cyclopentene. Both molecules have been extensively studied as photoswitches. 52,71-73 Both molecules show reversible and repeatable photoswitching in polymer matrices upon light irradiation.^{74–78} MC has a large molar absorption coefficient $(\sim 37,700 \text{ M}^{-1} \text{ cm}^{-1})^{79}$ at visible wavelengths and good solubility, enabling collective strong coupling in a microcavity. DAE, however, has a weaker absorption coefficient than MC (10,900 M⁻¹ cm⁻¹),80 making it more challenging to reach strong coupling in single-mode cavities. We focus our analysis on the reaction behavior of MC in the polaritonic strong coupling regime but also highlight measurements on DAE in the intermediate-to-weak-coupling regime to demonstrate that

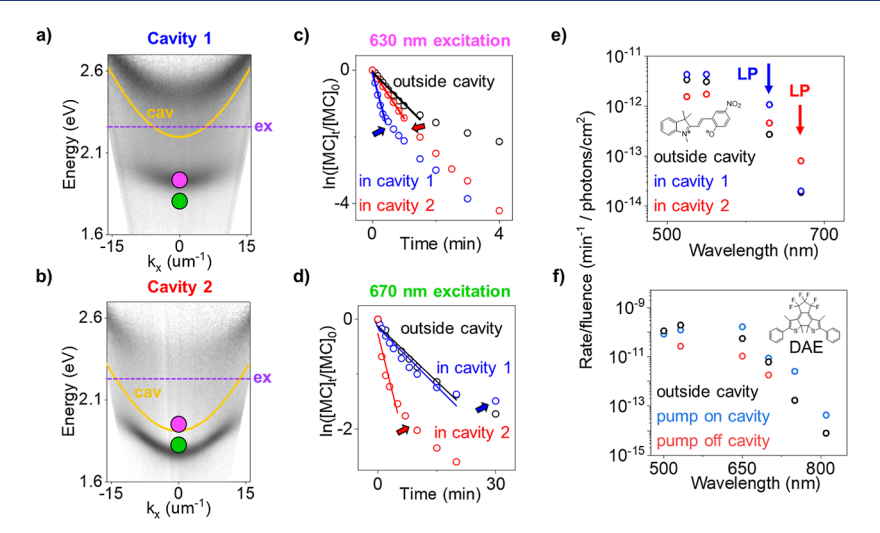


Figure 2. Photoisomerization kinetics as a function of excitation wavelength in MC and DAE. (a,b) Angle resolved reflection spectra of cavity 1 (a) with Ω_R = 517 meV and cavity 2 (b) with Ω_R = 605 meV. Pink dot represents 630 nm excitation at normal incidence; green dot represents 670 nm excitation at normal incidence. (c,d) Plots of reaction extent over time in control (black), cavity 1 (blue), and cavity 2 (red) for 630 nm excitation (c) and 670 nm excitation (d). Red and blue arrows positioned on the plots indicate the time point at which the system undergoes a transition from strong to weak coupling. The lines are fits to extract approximate isomerization rates in the strong-coupling regime. The cavities are gold cavities. Equivalent data is shown for silver cavities in Figure S6. (e,f) Fluence-normalized photoisomerization rate in each sample as a function of irradiation wavelength for MC (e) and DAE (f). The rate constants are extracted from single-exponential fits over the reaction times depicted in panels (c,d).

some effects on photoisomerization are not necessarily related to strong coupling.

To reach the strong-coupling regime, we disperse MC molecules in poly(methyl methacrylate) (PMMA) and embed them in a metallic Fabry-Perot cavity (Figure 1b, see Supporting Information, Section 1, for details). Silver mirrors are less lossy than gold mirrors but show signs of decomposition over long experimental times—we therefore carry out key measurements in both silver and gold cavities and report both sets of data, confirming that they show equivalent behavior. MC features a broad electronic absorption centered at approximately 550 nm (Figures 1c, S1, and S2). When MC is embedded in a resonant cavity, we observe a characteristic splitting of the exciton and photon peaks into upper and lower polariton bands (Figure 1c), in line with previous reports. 42,52,81 To resolve the polariton dispersion, we implement broadband Fourier-plane optical microscopy, enabling the capture of a full angle-resolved spectrum in a single (1 ms) exposure using low irradiation intensity (Figure S3). Compared to angle-resolved spectroscopy that requires beam- or sample-scanning, our approach crucially reduces light exposure, which would prevent accurate characterization of the dispersion evolution during a light-driven reaction. We confirm that this noninvasive approach leads to negligible photoinduced isomerization over a full experimental cycle in the absence of an additional light source driving photoisomerization (Figure S4). Although MC can revert to SP thermally in addition to light exposure, 42,52,79,85 Figure S4 also confirms that MC in PMMA is thermally stable over a full experimental cycle.

Figure 1d,e displays the polariton dispersion for the MC and colorless SP forms in a representative cavity, showing good agreement with simulations using the transfer matrix method (TMM) and the coupled oscillator model (COM). We obtain a Rabi splitting of $\Omega_R = 523$ meV in the MC form (obtained experimentally from the UP–LP separation in the absorbance spectrum at the anticrossing), similar to that achieved in previous reports. 42,52,81 Ω_R is larger than the full-width half-

maximum of both the cavity $\Gamma_c=114$ meV and the MC exciton band $\Gamma_{\rm MC}=447$ meV. Although different schemes are invoked to verify strong-coupling, for very broad/disordered molecular systems, such as MC, the condition $\Omega_{\rm R}>|\Gamma_{\rm c}-\Gamma_{\rm MC}|$ most closely matches secondary measures of strong coupling. Our system is therefore well within the strong-coupling regime at the onset of ultrastrong coupling ($\Omega_{\rm R}>0.2$ $E_0=450$ meV, where $E_0=2.25$ eV is the uncoupled molecular transition energy), although the validity of such analysis for ultrastrong coupling in highly disordered molecular systems is debated. So

Photoisomerization from MC to SP is induced using coherent light with tunable energy and in-plane momentum to target specific regions of the polariton dispersion (Figure S3). The evolution of the dispersion upon irradiation is then monitored over seconds to minutes. As MC molecules are converted to colorless SP, Rabi contraction 42,52 results in the LP (UP) branch shifting toward higher (lower) energy during the reaction (Figures 1f and S5). The evolution of the dispersion is compared to TMM calculations to extract the absolute concentration of MC over time, allowing for the determination of instantaneous photoisomerization rates in the cavity as a function of light-matter coupling strength, cavityexciton detuning, and irradiation energy and momentum. We will show that detailed analyses of photoisomerization kinetics, instead of overall yields, provide key indicators of subtle polariton-modified chemistry in our systems.

Absolute Photoisomerization Rate Enhancement is Driven by a Purcell Effect. We begin by comparing MC photoisomerization dynamics in three different environments: a strongly coupled system with the cavity energy crossing near the peak (90% of peak absorbance) of the MC electronic transition (cavity 1, Figure 2a); a strongly coupled system with the cavity detuned by -0.35 eV from the peak of the electronic transition (cavity 2, Figure 2b); and outside of the cavity (control). The cavity energies are tuned to be selectively resonant with different MC isomers (vide infra). The samples were irradiated with either 630 or 670 nm light, both at normal

incidence corresponding to momentum $k_x = 0$ (Figure 2a,b). To provide an estimate for the macroscopic reaction rate, we begin by assuming a simple first-order photoisomerization reaction from MC to SP (an assumption we revise with a more complete kinetic model below), with only the reactant (MC) absorbing at the excitation wavelengths. Thus

$$\frac{\mathrm{d}[\mathrm{MC}]_t}{\mathrm{d}t} = -k[\mathrm{MC}]_t, \qquad k = \sigma(\nu)I(\nu)\phi(\nu)$$
 for monochromatic light (1)

where $[MC]_t$ is the MC concentration at time t, k is the reaction rate constant, σ is the absorption cross section (proportional to A/[MC], where A is absorbance), ν is the irradiation frequency, I is the light irradiance, and ϕ is the reaction quantum yield. The integrated rate law, assuming k is constant, is simply $[MC]_t = [MC]_0 e^{-kt}$. Figure 2c,d plots $\ln \frac{[\text{MC}]_t - [\text{MC}]_{\infty}}{[\text{MC}]_0 - [\text{MC}]_{\infty}} = -kt$ for the two excitation conditions and the three environments, where $[MC]_{\infty}$ refers to a data point collected at late times, once the system has completely stopped evolving (indicating [MC] $_{\infty} \approx 0$). Arrows in Figure 2c,d point to the concentration at which the systems transition from strong to weak coupling. Most plots show a deviation from linear behavior, indicating nonfirst-order kinetics even prior to transitioning to weak coupling; we will show below that these deviations are key to understanding the effects of polaritons on our systems. For now, we estimate an average rate constant over the strong-coupling regime using the linear fits shown in Figure 2c,d.

Upon 630 nm irradiation, resonant with the LP of cavity 1 but not of cavity 2, we find that MC photoisomerization over the first minute of irradiation in cavity 1 is on average ~5 times faster than that of cavity 2 or in the control (Figure 2c). Analogous behavior is observed upon 670 nm irradiation, resonant with the LP of cavity 2 but not of cavity 1, which shows an ~4-fold enhancement of the photoisomerization rate in cavity 2 compared to cavity 1 or the control (Figure 2d). This symmetry between cavity 1 and cavity 2 suggests that the rate enhancement upon LP excitation is present over a large range of exciton-cavity detuning. Both the gold (Figure 2) and silver (Figure S6) cavities show equivalent behavior.

In contrast to these sizable rate modifications, the cavity appears to have little macroscopic effect on photoisomerization upon irradiation away from the LP branch, particularly when irradiating at energies lower than the LP (Figure 2d, compare black and blue data points). Furthermore, upon resonant excitation, the rate is drastically different only at early times, prior to substantial Rabi contraction; the latter shifts the LP branch energy away from the excitation energy, at which point the rate approximately recovers that of the control sample outside the cavity. Thus, our results indicate that it is mainly upon the resonant excitation of a polariton branch that we substantially enhance photoisomerization rates. These findings are summarized in Figure 2e, where we plot the irradiation fluence-normalized reaction rate constants for the control and two cavities for different excitation wavelengths extracted using linear fits over the strong-coupling regime. The figure emphasizes that the most significant effect is rate enhancement compared to the control when the excitation is resonant with the LP. Fluence-dependent measurements provide confidence that the observed effects are not due to thermally induced photoisomerization arising from light-induced heating (Figures

S7 and S8).87 Instead, this overall rate enhancement effect can be understood as arising from a cavity-induced renormalization of the photonic density of states, as was recently inferred for different reactions. 56,88 This effect does not require strong light-matter coupling. Nevertheless, our results indicate that enhanced absorption at the LP branch followed by conversion of LPs into dark states does enable more efficient use of photons resonant with the LP branch compared to that outside the cavity. Thus, the cavity allows the use of lower-energy light to drive photoisomerization, in essence red-shifting the onset of photochemistry. 41 We return below to absorptionnormalized measurements to more sensitively tease out polaritonic effects.

To test the effect of strong versus weak coupling as well as generalize our result to a different photoswitch, we carry out identical measurements using DAE in an intermediate-toweakly coupled cavity (Figure S9). We show the fluencenormalized reaction rates for DAE in Figure 2f, comparing rates outside the cavity versus inside the cavity at different wavelengths. Given the steep cavity dispersion, we add an additional control parameter where we selectively pump on or off a cavity mode by changing the angle (or momentum) of irradiation (Figure S3), enabling a more thorough characterization of the effect of the cavity at all wavelengths. At energies below the absorption peak of bare DAE (Figure S1), resonant irradiation of the cavity causes a rate enhancement effect similar to that of the MC data (compare Figure 2e,f). In addition, in DAE microcavities, we observe rate suppression when pumping off of the cavity mode for any given wavelength (Figures 2e and S9); this rate suppression is simply a result of lower system absorbance at these wavelengths due to the cavity. Overall, our results show that the most evident macroscopic changes to photoisomerization kinetics observed when embedding molecules within microcavities primarily stem from a renormalized density of photonic states, present in both weak- and strong-coupling regimes.

Kinetic Competition between Polariton Localization and Cavity Losses Leads to Yield Suppression. To remove the effect of renormalized system absorbance due to the cavity, we now account for time-dependent changes in σ (eq 1) in the cavities to calculate the yield enhancement or suppression factor $\gamma = \langle \frac{\phi_{\rm cavity}}{\phi_{\rm control}} \rangle_{\rm SC}$ for each excitation condition in MC, where the brackets indicate averaging over data collected only within the strong-coupling regime (details and normalization method comparison in Supporting Information, Section 2.4 and Figure S10). The values of γ are tabulated in Figure 3a for two different cavities, color-coded to the excitation conditions shown in Figure 3b,c. We also tabulate absolute rate enhancements RE = $\frac{k_{\text{cavity}}}{k_{\text{control}}}$ for comparison, using the rates from Figure 2e. We observe photoisomerization yield suppression (γ < 1) in all cases. We find that the highest photoisomerization yield occurs when the cavity samples are excited at 550 nm, near the resonance peak of the uncoupled molecular transition. Figure 3d overlaps the extracted γ values for the two cavities at each excitation wavelength with the bare MC absorbance. The plot shows that although the absolute isomerization rate increases when pumping polariton resonances (Figure 2e), γ decreases monotonically as we detune the excitation away from the bare molecular resonance (Figure 3d).

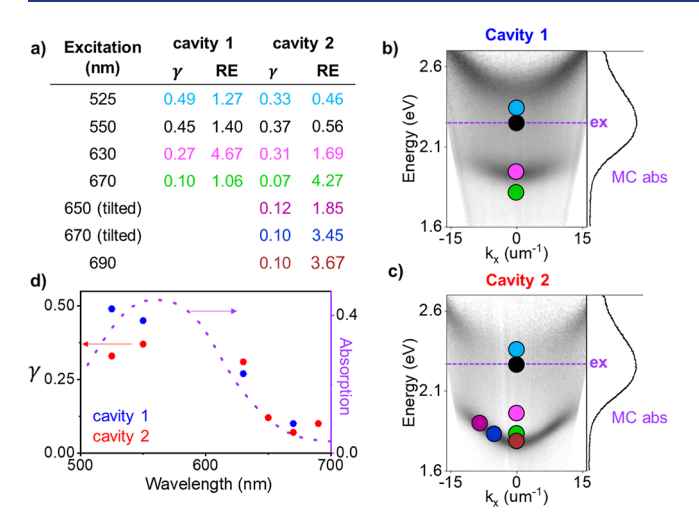


Figure 3. Cavity-induced photoisomerization yield suppression in MC. (a) Absorption-normalized yield enhancement (γ , see text for calculation details). The absolute rate enhancements (RE, which are normalized for fluence but not absorbance) from Figure 2e are also tabulated for comparison. (b,c) Angle-resolved reflection spectra of cavities 1 and 2, respectively. Each dot represents a different excitation condition in energy and momentum, color-coded to panel (a). (d) Plot of γ vs excitation wavelength, showing that γ approximately follows molecular absorbance as a function of wavelength.

Multiple studies have shown that relaxation dynamics in molecular polaritons are dominated by dark states. 62,89,90 Indeed, excitation into any state (UP, LP, or dark states) tends to localize both spatially and energetically into the dark state

manifold because of the latter's large density of states. 49,59,63,91 This aspect is particularly relevant in molecular polaritons with large disorder, since the latter ensures energetic overlap between polariton branches and molecular states over a large range of detunings. ^{89,90} The trend we observe in γ (Figure 3d) can be rationalized within this context and suggests that photochemistry in our systems is principally driven by (relatively) localized dark states: as the detuning between the excitation and bare exciton resonance increases, we expect a smaller LP \rightarrow dark state transfer rate. The other decay pathway for LPs is to the ground state, typically on sub-100 fs time scales, dictated primarily by cavity losses. Given this kinetic competition between polariton localization into dark states and polariton decay to the ground state, large detuning (small LP \rightarrow dark state rate) results in a lower dark state yield and thus lower photochemical yields (Figure 3d). Therefore, cavity coupling, particularly under conditions where the LP is significantly detuned from dark states through ultrastrong coupling or large detuning, can yield photoisomerization suppression even without fundamentally modifying molecular potential surfaces. 41,88 We emphasize, however, that the absolute photoisomerization rate enhancement (per irradiation photon rather than absorbed photon, RE in Figure 3a) can be large in microcavities since it allows low-energy light below the molecular resonance to be efficiently absorbed by the system and transferred into reactive dark states.

Polariton Funneling to Target Reactants Allows Steering Chemical Reactivity in Isomer Mixtures. Finally, we turn to a sought-after polaritonic effect: control over reaction selectivity through strong light-matter coupling. It is well understood that cavity coupling facilitates long-range wave

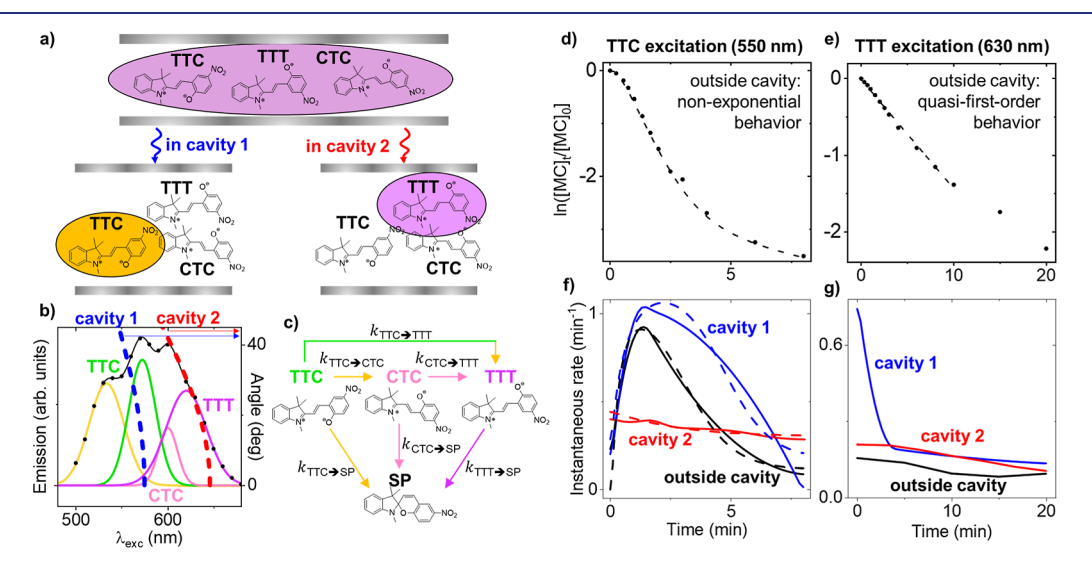


Figure 4. Polaritonic funneling to target MC isomers. (a) Diagram depicting initially delocalized polaritons localizing onto specific MC isomers upon decoherence. The isomer into which polaritons localize depends on exciton-cavity detuning. (b) Photoluminescence excitation spectrum of MC in PMMA outside the cavity. The spectrum reveals four different isomers, which we model with Gaussian functions with dominant contributions from TTC, CTC, and TTT isomers. The bare photonic dispersions of cavity 1 (blue) and cavity 2 (red) are overlaid with the excitation spectrum, displaying preferential spectral overlap of cavity 1 with TTC isomers and of cavity 2 with TTT isomers. (c) Schematic of the rate equations used to model the isomerization kinetics of our system between different MC isomers and SP. (d,e) Photoisomerization kinetics of MC in PMMA outside the cavity following 550 nm (d, mostly TTC) and 630 nm (e, mostly TTT) excitation. (f,g) Instantaneous rate of reaction over time plotted for 550 nm excitation (f) and 630 nm excitation (g) for the control, gold cavity 1, and gold cavity 2. Solid curves depict experimental data; dashed curves depict the best fit using the kinetic model depicted in panel (c), with extracted rate constants shown in Table S1. TTC-dominated kinetics exhibits a characteristic rise-and-fall feature in the instantaneous rate, indicating nonexponential behavior. TTT-dominated kinetics is nearly monoexponential. Panel (f) indicates switching from TTC- to TTT-dominated kinetics by increasing exciton-cavity detuning. Raw data for both gold and silver cavities are shown in Figure S11. Note that these data sets are collected with 10-fold lower fluence than Figure 2 data to allow finer temporal sampling of the kinetic evolution.

function delocalization and transport. 9-15 When the cavity couples to multiple partially overlapping optical transitions, the polariton delocalizes across different species and facilitates energy transfer between them. 54,68,70,92 In the context of chemical reactions, we posit that this delocalization can help funnel energy⁶⁸ to target reactants and thus steer chemical reactivity in reaction mixtures (Figure 4a). Related mechanisms of cavity-mediated intramolecular energy redistribution of thermal excitations have recently been postulated to account for modified ground-state chemical reactions under vibrational strong coupling.⁹³

There are four stable isomers of MC. The two isomers known to dominate absorption are trans-trans-cis (TTC) and trans-trans (TTT) (Figure 4a), which adopt different photoisomerization pathways. These isomers have partially overlapping absorption spectra that can be distinguished through photoluminescence excitation spectroscopy 94,96 (PLE, Figure 4b). PLE of our control sample (MC in a PMMA matrix outside the cavity) distinguishes up to four isomers, modeled with four Gaussian functions in Figure 4b. Isomer assignment is debated in the literature, 94,96,98-100 but given the known dominating contributions of TTC and TTT to PLE spectra, we assign the main peaks at 570 and 618 nm to TTC and TTT, respectively, in agreement with assignments for MC in solution. 96,101 TTC is the most stable isomer and is expected to be in the largest concentration, but TTT has a much higher photoluminescence quantum yield, explaining the large TTT peak in PLE spectra.96 The other peaks are likely CTC and CTT, with CTC known to be involved in the excited-state isomerization pathway. 94 We call the middle isomer CTC from hereon for simplicity, but note that isomer assignment is irrelevant to the discussion that follows. The bare cavity photon dispersions of cavity 1 and cavity 2 are overlaid on the PLE spectrum in Figure 4b. Both cavities spectrally overlap with multiple isomers but display preferential overlap of cavity 1 with TTC and of cavity 2 with TTT. Our central question is whether, upon decoherence, polaritons localize into a specific isomer selected by the cavity resonance, despite initially exciting the whole mixture (Figure 4a). This process would allow steering photoexcitations toward a particular reaction pathway irrespective of excitation condition, thus offering the possibility to harvest photons efficiently through the whole mixture and direct them toward a particular product state—an approach to enhancing chemical rates while controlling selectivity in reaction mixtures.

Prior studies in solution have demonstrated excited-state photoisomerization among ring-open isomers, specifically TTC \to TTT, TTC \to CTC, and CTC \to TTT, 94,96 in addition to the ring-closing reactions to SP (Figure 4c). Indeed, we find that in our control samples (outside the cavity), exciting mainly TTC isomers at 550 nm results in nonexponential behavior (Figure 4d), whereas exciting TTT isomers at 630 nm results in quasi-monoexponential isomerization kinetics (Figure 4e), as indicated by the linear fit (dashed line) over the first 10 min. These data support the notion that TTT isomers excited with 630 nm light convert only to SP, resulting in firstorder kinetics, whereas 550 nm excitation results in branching to multiple isomers that also absorb light and undergo ringclosing at different rates. We develop a model according to Figure 4c (Supporting Information, Section 3), and we confirm that a minimum of three ring-open MC isomers are required to reproduce the observed kinetics for 550 nm excitation. The fit from the model is shown as a dashed line in Figure 4d

(extracted parameters are given in Table S1) and captures all essential features of the data.

The photoisomerization kinetics for all systems is summarized in Figure 4f,g, which plots the instantaneous photoisomerization rate, defined as $k_{\text{inst}} = -\frac{\partial}{\partial t} \ln \left(\frac{[\text{MC}]_t}{[\text{MC}]_0} \right)$ Plotting this derivative emphasizes subtle deviations from first-order kinetics (the raw data are shown in Figure S11). Outside the cavity, excitation at 550 nm results in a characteristic rise-and-fall profile in k_{inst} , whereas excitation at 630 nm results in an almost constant k_{inst} , the latter indicating quasi-first-order kinetics. We use this clear distinction in the isomerization kinetics as an indicator of the dominant photoisomerization pathway in the cavities.

Our key results are shown in Figure 4f. Upon 550 nm excitation (resonant primarily with TTC), cavity 1 shows a rise-and-fall profile in k_{inst} , consistent with that of the outsidecavity sample. We therefore assign this behavior to TTCdominated isomerization in cavity 1 upon 550 nm excitation. The small difference between cavity 1 and control kinetics is captured by our model primarily through a reduction in the rate of TTC → TTT in cavity 1, suggesting that cavity 1 favors localization of the excitation onto TTC isomers (Table S1). In contrast, our most important result is that for identical 550 nm excitation conditions, cavity 2 exhibits simple dynamics approaching monoexponential behavior, characteristic of TTT isomer dynamics (the red trace in Figure 4f is similar to the black trace in Figure 4g). This observation indicates that, remarkably, the polariton that is presumably initially delocalized across multiple isomers localizes specifically into TTT isomers upon decoherence, selectively triggering ringclosing from TTT. Our model captures this switch to TTTdominated dynamics in cavity 2 upon 550 nm excitation by either: (i) Massively increasing the TTC \rightarrow TTT and CTC \rightarrow TTT rates (Table S2, fits shown in Figure S12), implying a cavity modification of photoisomerization rate; or (ii) Shifting the initial population from TTC to CTC and TTT (Table S1, fits shown in Figure 4f), implying a modification of system eigenstates resulting in a different initial condition upon 550 nm excitation. In both cases, these results show that tuning the cavity to be resonant with one subpopulation of isomers allows efficient funneling of photoexcitations into those isomers.

Complementary angle-resolved photoluminescence (PL) measurements (Figure S13) support our interpretation. Upon 550 nm excitation, the PL intensity in cavity 1 is \sim 2 times lower than outside the cavity, but the PL spectrum is almost identical, suggesting that cavity 1 has little effect on the relative isomer fractions upon 550 nm excitation. In cavity 2, however, the PL intensity is ~6 times larger than that in cavity 1 for identical excitation conditions. The PL is also red-shifted, with light emitted primarily through the LP of cavity 2. Given the larger PL quantum yield of TTT compared to TTC, 96 these results support the notion that photoexcitations are selectively funneled to TTT in cavity 2. Nevertheless, we note that the interpretation of PL intensity and spectrum is complicated by effects such as radiative pumping of the LP by relaxed molecular states and Purcell enhancement, which may account for the features observed in the PL. We therefore posit that monitoring chemical kinetics, which is independent of light outcoupling, is a superior approach to identifying polariton-mediated energy funneling and localization dynamics in our system.

Finally, upon 630 nm excitation (resonant primarily with TTT isomers and with the LP of cavity 1 at k=0), cavity 2 continues to exhibit TTT kinetics (Figure 4g), matching the kinetics of the outside-cavity sample, as expected. Cavity 1 displays an initially large isomerization rate due to resonant excitation of the LP at 630 nm (Figures 4g and 2e); however, following Rabi contraction, the excitation wavelength is subresonant with the LP, resulting in primarily TTT excitation and monoexponential kinetics, consistent with cavity 2 and the control.

Overall, these results show that polaritons in cavity 2 systematically localize into the TTT isomer, even upon excitation at wavelengths normally resonant with TTC isomers, resulting in TTT-dominated isomerization kinetics. Thus, appropriate tuning of the cavity resonance steers excitedstate reaction pathways in chemical mixtures by funneling the absorbed energy toward a target reactant state, similar to lightharvesting schemes, though the overall photon efficiency limits of this process in cavities remains to be investigated. These results suggest that strong light-matter coupling in chemical mixtures allows steering chemical dynamics in a potentially more profound way than by acting as an optical filter, which was recently suggested to be the case for chemical systems with single-component reactants. 56,88,102 This approach will be particularly valuable to adopt in mixtures of reactants that have drastically different photochemical pathways and product states. Electronic strong-coupling in this context would provide a compelling platform to achieve precise reaction specificity, product selectivity, including suppression of undesired products, and reconfigurable photoswitching.

CONCLUSIONS

Overall, we have disentangled three effects that contribute to the cavity-modified photoisomerization kinetics of a photoswitch when the reactant's electronic excitation is strongly coupled to the photonic cavity mode. Our results indicate that cavity coupling can influence the efficiency, rate, and selectivity of chemical reactions through kinetic competition and polariton-assisted energy transfer in reaction mixtures. First, the most obvious macroscopic effect of the cavity is a Purcelllike renormalization of the photonic density of states that leads to enhanced absorption at wavelengths resonant with the polariton or cavity modes. This effect is not polaritonic in nature but does lead to an absolute rate enhancement per irradiation photon at some wavelengths, notably allowing redshifting of the onset of photoisomerization. Second, when normalized for the number of absorbed photons, our results indicate that cavity strong coupling decreases the photoisomerization yields. The yield suppression becomes more dramatic as the excitation wavelength is detuned from the bare molecular absorbance. We assign the observed behavior to a smaller polariton \rightarrow dark state population transfer upon larger excitation detuning; combined with cavity losses, this effect results in overall yield suppression. Finally, and most excitingly, we observe polariton-assisted selectivity over the reaction paths. This behavior is observed in a reaction mixture containing multiple isomers with partially overlapping but distinct electronic transitions. When the cavity is tuned into resonance with a target reactant isomer, our results show that polaritons that are initially delocalized across the reaction mixture localize into the target state, irrespective of initial excitation conditions. These results suggest that the energy absorbed by the reaction mixture can be funneled to a target

reactant. Such polariton funneling provides an enticing prospect for steering photochemical reactions in complex mixtures toward desired chemical products with high efficiency.

ASSOCIATED CONTENT

5 Supporting Information

The Supporting Information is available free of charge at https://pubs.acs.org/doi/10.1021/jacs.3c11292.

Materials and methods, primary data on Rabi contraction, additional data on silver cavities and diarylethene cavities, fluence-dependent photoisomerization, details of kinetic models, and angle-resolved photoluminescence data (PDF)

AUTHOR INFORMATION

Corresponding Author

Milan Delor — Department of Chemistry, Columbia University, New York, New York 10027, United States; orcid.org/0000-0002-9480-9235; Email: milan.delor@columbia.edu

Authors

 Inki Lee - Department of Chemistry, Columbia University, New York, New York 10027, United States
 Sarah R. Melton - Department of Chemistry, Columbia University, New York, New York 10027, United States
 Ding Xu - Department of Chemistry, Columbia University, New York, New York 10027, United States

Complete contact information is available at: https://pubs.acs.org/10.1021/jacs.3c11292

Notes

The authors declare no competing financial interest.

ACKNOWLEDGMENTS

We thank Yuzuka Karube for help in collecting linear absorption spectra and Dr. Arkajit Mandal for helpful discussions. This material is based upon work supported by the National Science Foundation under grant number CHE-2203844, and by the Arnold and Mabel Beckman Foundation through a Beckman Young Investigator award. We acknowledge the use of the Columbia University shared facilities and instrumentation, specifically the electron beam evaporator, supported by the National Science Foundation through the Columbia Nano Initiative and the Materials Research Science and Engineering Center DMR-2011738.

REFERENCES

- (1) Mills, D. L.; Burstein, E. Polaritons: The Electromagnetic Modes of Media. *Rep. Prog. Phys.* **1974**, *37*, 817–926.
- (2) Hopfield, J. J. Theory of the Contribution of Excitons to the Complex Dielectric Constant of Crystals. *Phys. Rev.* **1958**, *112*, 1555–1567.
- (3) Herrera, F.; Owrutsky, J. Molecular Polaritons for Controlling Chemistry with Quantum Optics. *J. Chem. Phys.* **2020**, *152*, 100902.
- (4) Feist, J.; Galego, J.; Garcia-Vidal, F. J. Polaritonic Chemistry with Organic Molecules. *ACS Photonics* **2018**, *5*, 205–216.
- (5) Mandal, A.; Taylor, M. A. D.; Weight, B. M.; Koessler, E. R.; Li, X.; Huo, P. Theoretical Advances in Polariton Chemistry and Molecular Cavity Quantum Electrodynamics. *Chem. Rev.* **2023**, *123*, 9786–9879.

- (6) Dunkelberger, A. D.; Simpkins, B. S.; Vurgaftman, I.; Owrutsky, J. C. Vibration-Cavity Polariton Chemistry and Dynamics. *Annu. Rev. Phys. Chem.* **2022**, *73*, 429–451.
- (7) Nagarajan, K.; Thomas, A.; Ebbesen, T. W. Chemistry under Vibrational Strong Coupling. *J. Am. Chem. Soc.* **2021**, *143*, 16877–16889.
- (8) Weisbuch, C.; Nishioka, M.; Ishikawa, A.; Arakawa, Y. Observation of the Coupled Exciton-Photon Mode Splitting in a Semiconductor Quantum Microcavity. *Phys. Rev. Lett.* **1992**, *69*, 3314–3317.
- (9) Steger, M.; Liu, G.; Nelsen, B.; Gautham, C.; Snoke, D. W.; Balili, R.; Pfeiffer, L.; West, K. Long-Range Ballistic Motion and Coherent Flow of Long-Lifetime Polaritons. *Phys. Rev. B* **2013**, 88, 235314.
- (10) Orgiu, E.; George, J.; Hutchison, J. A.; Devaux, E.; Dayen, J. F.; Doudin, B.; Stellacci, F.; Genet, C.; Schachenmayer, J.; Genes, C.; Pupillo, G.; Samorì, P.; Ebbesen, T. W. Conductivity in Organic Semiconductors Hybridized with the Vacuum Field. *Nat. Mater.* **2015**, *14*, 1123–1129.
- (11) Hou, S.; Khatoniar, M.; Ding, K.; Qu, Y.; Napolov, A.; Menon, V. M.; Forrest, S. R. Ultralong-Range Energy Transport in a Disordered Organic Semiconductor at Room Temperature Via Coherent Exciton-Polariton Propagation. *Adv. Mater.* **2020**, 32, 2002127.
- (12) Balasubrahmaniyam, M.; Simkhovich, A.; Golombek, A.; Sandik, G.; Ankonina, G.; Schwartz, T. From Enhanced Diffusion to Ultrafast Ballistic Motion of Hybrid Light-Matter Excitations. *Nat. Mater.* **2023**, 22, 338–344.
- (13) Xu, D.; Mandal, A.; Baxter, J. M.; Cheng, S.-W.; Lee, I.; Su, H.; Liu, S.; Reichman, D. R.; Delor, M. Ultrafast Imaging of Polariton Propagation and Interactions. *Nat. Commun.* **2023**, *14*, 3881.
- (14) Pandya, R.; Ashoka, A.; Georgiou, K.; Sung, J.; Jayaprakash, R.; Renken, S.; Gai, L.; Shen, Z.; Rao, A.; Musser, A. J. Tuning the Coherent Propagation of Organic Exciton-Polaritons through Dark State Delocalization. *Adv. Sci.* **2022**, *9*, 2105569.
- (15) Myers, D. M.; Mukherjee, S.; Beaumariage, J.; Snoke, D. W.; Steger, M.; Pfeiffer, L. N.; West, K. Polariton-Enhanced Exciton Transport. *Phys. Rev. B* **2018**, *98*, 235302.
- (16) Bloch, J.; Carusotto, I.; Wouters, M. Non-Equilibrium Bose–Einstein Condensation in Photonic Systems. *Nat. Rev. Phys.* **2022**, *4*, 470–488.
- (17) Kasprzak, J.; Richard, M.; Kundermann, S.; Baas, A.; Jeambrun, P.; Keeling, J. M. J.; Marchetti, F. M.; Szymańska, M. H.; André, R.; Staehli, J. L.; Savona, V.; Littlewood, P. B.; Deveaud, B.; Dang, L. S. Bose–Einstein Condensation of Exciton Polaritons. *Nature* **2006**, 443, 409–414.
- (18) Su, R.; Ghosh, S.; Wang, J.; Liu, S.; Diederichs, C.; Liew, T. C. H.; Xiong, Q. Observation of Exciton Polariton Condensation in a Perovskite Lattice at Room Temperature. *Nat. Phys.* **2020**, *16*, 301–306.
- (19) Imamoglu, A.; Schmidt, H.; Woods, G.; Deutsch, M. Strongly Interacting Photons in a Nonlinear Cavity. *Phys. Rev. Lett.* **1997**, 79, 1467–1470.
- (20) Delteil, A.; Fink, T.; Schade, A.; Höfling, S.; Schneider, C.; İmamoğlu, A. Towards Polariton Blockade of Confined Exciton-Polaritons. *Nat. Mater.* **2019**, *18*, 219–222.
- (21) Muñoz-Matutano, G.; Wood, A.; Johnsson, M.; Vidal, X.; Baragiola, B. Q.; Reinhard, A.; Lemaître, A.; Bloch, J.; Amo, A.; Nogues, G.; Besga, B.; Richard, M.; Volz, T. Emergence of Quantum Correlations from Interacting Fibre-Cavity Polaritons. *Nat. Mater.* **2019**, *18*, 213–218.
- (22) Cuevas, Á.; López Carreño, J. C.; Silva, B.; De Giorgi, M.; Suárez-Forero, D. G.; Sánchez Muñoz, C.; Fieramosca, A.; Cardano, F.; Marrucci, L.; Tasco, V.; Biasiol, G.; del Valle, E.; Dominici, L.; Ballarini, D.; Gigli, G.; Mataloni, P.; Laussy, F. P.; Sciarrino, F.; Sanvitto, D. First Observation of the Quantized Exciton-Polariton Field and Effect of Interactions on a Single Polariton. *Sci. Adv.* 2018, 4, No. eaao6814.

- (23) Zasedatelev, A. V.; Baranikov, A. V.; Sannikov, D.; Urbonas, D.; Scafirimuto, F.; Shishkov, V. Y.; Andrianov, E. S.; Lozovik, Y. E.; Scherf, U.; Stöferle, T.; Mahrt, R. F.; Lagoudakis, P. G. Single-Photon Nonlinearity at Room Temperature. *Nature* **2021**, *597*, 493–497.
- (24) Garcia-Vidal, F. J.; Ciuti, C.; Ebbesen, T. W. Manipulating Matter by Strong Coupling to Vacuum Fields. *Science* **2021**, *373*, No. eabd0336.
- (25) Hertzog, M.; Wang, M.; Mony, J.; Börjesson, K. Strong Light-Matter Interactions: A New Direction within Chemistry. *Chem. Soc. Rev.* **2019**, *48*, 937–961.
- (26) Li, T. E.; Cui, B.; Subotnik, J. E.; Nitzan, A. Molecular Polaritonics: Chemical Dynamics Under Strong Light-Matter Coupling. *Annu. Rev. Phys. Chem.* **2022**, *73*, 43–71.
- (27) Ribeiro, R. F.; Martínez-Martínez, L. A.; Du, M.; Campos-Gonzalez-Angulo, J.; Yuen-Zhou, J. Polariton Chemistry: Controlling Molecular Dynamics with Optical Cavities. *Chem. Sci.* **2018**, *9*, 6325–6339.
- (28) Thomas, A.; Lethuillier-Karl, L.; Nagarajan, K.; Vergauwe, R. M. A.; George, J.; Chervy, T.; Shalabney, A.; Devaux, E.; Genet, C.; Moran, J.; Ebbesen, T. W. Tilting a Ground-State Reactivity Landscape by Vibrational Strong Coupling. *Science* **2019**, *363*, 615–619.
- (29) Ahn, W.; Triana, J. F.; Recabal, F.; Herrera, F.; Simpkins, B. S. Modification of Ground-State Chemical Reactivity via Light-Matter Coherence in Infrared Cavities. *Science* **2023**, *380*, 1165–1168.
- (30) Imperatore, M. V.; Asbury, J. B.; Giebink, N. C. Reproducibility of Cavity-Enhanced Chemical Reaction Rates in the Vibrational Strong Coupling Regime. *J. Chem. Phys.* **2021**, *154*, 191103.
- (31) Wiesehan, G. D.; Xiong, W. Negligible Rate Enhancement from Reported Cooperative Vibrational Strong Coupling Catalysis. *J. Chem. Phys.* **2021**, *155*, 241103.
- (32) Gao, F.; Guo, J.; Si, Q.; Wang, L.; Zhang, F.; Yang, F. Modification of ATP Hydrolysis by Strong Coupling with O-H Stretching Vibration. *ChemPhotoChem* **2023**, 7, No. e202200330.
- (33) Mandal, A.; Huo, P. Investigating New Reactivities Enabled by Polariton Photochemistry. *J. Phys. Chem. Lett.* **2019**, *10*, 5519–5529.
- (34) Vurgaftman, I.; Simpkins, B. S.; Dunkelberger, A. D.; Owrutsky, J. C. Negligible Effect of Vibrational Polaritons on Chemical Reaction Rates via the Density of States Pathway. *J. Phys. Chem. Lett.* **2020**, *11*, 3557–3562.
- (35) Du, M.; Yuen-Zhou, J. Catalysis by Dark States in Vibropolaritonic Chemistry. *Phys. Rev. Lett.* **2022**, *128*, 096001.
- (36) Mandal, A.; Li, X.; Huo, P. Theory of Vibrational Polariton Chemistry in the Collective Coupling Regime. *J. Chem. Phys.* **2022**, *156*, 014101.
- (37) Galego, J.; Climent, C.; Garcia-Vidal, F. J.; Feist, J. Cavity Casimir-Polder Forces and Their Effects in Ground-State Chemical Reactivity. *Phys. Rev. X* **2019**, *9*, 021057.
- (38) Campos-Gonzalez-Angulo, J. A.; Yuen-Zhou, J. Polaritonic Normal Modes in Transition State Theory. *J. Chem. Phys.* **2020**, *152*, 161101.
- (39) Munkhbat, B.; Wersäll, M.; Baranov, D. G.; Antosiewicz, T. J.; Shegai, T. Suppression of Photo-Oxidation of Organic Chromophores by Strong Coupling to Plasmonic Nanoantennas. *Sci. Adv.* **2018**, *4*, No. eaas9552.
- (40) Peters, V. N.; Faruk, M. O.; Asane, J.; Alexander, R.; Peters, D. A.; Prayakarao, S.; Rout, S.; Noginov, M. A. Effect of Strong Coupling on Photodegradation of the Semiconducting Polymer P3HT. *Optica* **2019**, *6*, 318.
- (41) Mony, J.; Climent, C.; Petersen, A. U.; Moth-Poulsen, K.; Feist, J.; Börjesson, K. Photoisomerization Efficiency of a Solar Thermal Fuel in the Strong Coupling Regime. *Adv. Funct. Mater.* **2021**, *31*, 2010737.
- (42) Hutchison, J. A.; Schwartz, T.; Genet, C.; Devaux, E.; Ebbesen, T. W. Modifying Chemical Landscapes by Coupling to Vacuum Fields. *Angew. Chem., Int. Ed.* **2012**, *51*, 1592–1596.
- (43) Gu, B.; Mukamel, S. Optical-Cavity Manipulation of Conical Intersections and Singlet Fission in Pentacene Dimers. *J. Phys. Chem. Lett.* **2021**, *12*, 2052–2056.

- (44) Martínez-Martínez, L. A.; Du, M.; Ribeiro, R. F.; Kéna-Cohen, S.; Yuen-Zhou, J. Polariton-Assisted Singlet Fission in Acene Aggregates. J. Phys. Chem. Lett. 2018, 9, 1951–1957.
- (45) Climent, C.; Casanova, D.; Feist, J.; Garcia-Vidal, F. J. Not Dark yet for Strong Light-Matter Coupling to Accelerate Singlet Fission Dynamics. *Cell Rep. Phys. Sci.* **2022**, *3*, 100841.
- (46) Galego, J.; Garcia-Vidal, F. J.; Feist, J. Suppressing Photochemical Reactions with Quantized Light Fields. *Nat. Commun.* **2016**, 7, 13841.
- (47) Galego, J.; Garcia-Vidal, F. J.; Feist, J. Cavity-Induced Modifications of Molecular Structure in the Strong-Coupling Regime. *Phys. Rev. X* **2015**, *5*, 041022.
- (48) Herrera, F.; Spano, F. C. Cavity-Controlled Chemistry in Molecular Ensembles. *Phys. Rev. Lett.* **2016**, *116*, 238301.
- (49) Scholes, G. D.; DelPo, C. A.; Kudisch, B. Entropy Reorders Polariton States. J. Phys. Chem. Lett. 2020, 11, 6389-6395.
- (50) Yu, Y.; Mallick, S.; Wang, M.; Börjesson, K. Barrier-Free Reverse-Intersystem Crossing in Organic Molecules by Strong Light-Matter Coupling. *Nat. Commun.* **2021**, *12*, 3255.
- (51) Stranius, K.; Hertzog, M.; Börjesson, K. Selective Manipulation of Electronically Excited States through Strong Light-Matter Interactions. *Nat. Commun.* **2018**, *9*, 2273.
- (52) Schwartz, T.; Hutchison, J. A.; Genet, C.; Ebbesen, T. W. Reversible Switching of Ultrastrong Light-Molecule Coupling. *Phys. Rev. Lett.* **2011**, *106*, 196405.
- (53) Polak, D.; Jayaprakash, R.; Lyons, T. P.; Martínez-Martínez, L. Á.; Leventis, A.; Fallon, K. J.; Coulthard, H.; Bossanyi, D. G.; Georgiou, K.; Petty II, A. J.; Anthony, J.; Bronstein, H.; Yuen-Zhou, J.; Tartakovskii, A. I.; Clark, J.; Musser, A. J. Manipulating Molecules with Strong Coupling: Harvesting Triplet Excitons in Organic Exciton Microcavities. *Chem. Sci.* **2020**, *11*, 343–354.
- (54) Dovzhenko, D.; Lednev, M.; Mochalov, K.; Vaskan, I.; Rakovich, Y.; Karaulov, A.; Nabiev, I. Polariton-Assisted Manipulation of Energy Relaxation Pathways: Donor-Acceptor Role Reversal in a Tuneable Microcavity. *Chem. Sci.* **2021**, *12*, 12794–12805.
- (55) Zeng, H.; Pérez-Sánchez, J. B.; Eckdahl, C. T.; Liu, P.; Chang, W. J.; Weiss, E. A.; Kalow, J. A.; Yuen-Zhou, J.; Stern, N. P. Control of Photoswitching Kinetics with Strong Light-Matter Coupling in a Cavity. J. Am. Chem. Soc. 2023, 145, 19655–19661.
- (56) Thomas, P. A.; Tan, W. J.; Kravets, V. G.; Grigorenko, A. N.; Barnes, W. L. Non-Polaritonic Effects in Cavity-Modified Photochemistry. *Adv. Mater.* **2023**, *36*, 2309393.
- (57) Canaguier-Durand, A.; Devaux, E.; George, J.; Pang, Y.; Hutchison, J. A.; Schwartz, T.; Genet, C.; Wilhelms, N.; Lehn, J.-M.; Ebbesen, T. W. Thermodynamics of Molecules Strongly Coupled to the Vacuum Field. *Angew. Chem., Int. Ed.* **2013**, *52*, 10533–10536.
- (58) Schwartz, T.; Hutchison, J. A.; Léonard, J.; Genet, C.; Haacke, S.; Ebbesen, T. W. Polariton Dynamics under Strong Light-Molecule Coupling. *ChemPhysChem* **2013**, *14*, 125–131.
- (59) Tichauer, R. H.; Feist, J.; Groenhof, G. Multi-Scale Dynamics Simulations of Molecular Polaritons: The Effect of Multiple Cavity Modes on Polariton Relaxation. *J. Chem. Phys.* **2021**, *154*, 104112.
- (60) Virgili, T.; Coles, D.; Adawi, A. M.; Clark, C.; Michetti, P.; Rajendran, S. K.; Brida, D.; Polli, D.; Cerullo, G.; Lidzey, D. G. Ultrafast Polariton Relaxation Dynamics in an Organic Semi-conductor Microcavity. *Phys. Rev. B* **2011**, *83*, 245309.
- (61) Coles, D. M.; Grant, R. T.; Lidzey, D. G.; Clark, C.; Lagoudakis, P. G. Imaging the Polariton Relaxation Bottleneck in Strongly Coupled Organic Semiconductor Microcavities. *Phys. Rev. B* **2013**, *88*, 121303.
- (62) Groenhof, G.; Climent, C.; Feist, J.; Morozov, D.; Toppari, J. J. Tracking Polariton Relaxation with Multiscale Molecular Dynamics Simulations. *J. Phys. Chem. Lett.* **2019**, *10*, 5476–5483.
- (63) Renken, S.; Pandya, R.; Georgiou, K.; Jayaprakash, R.; Gai, L.; Shen, Z.; Lidzey, D. G.; Rao, A.; Musser, A. J. Untargeted Effects in Organic Exciton-Polariton Transient Spectroscopy: A Cautionary Tale. *J. Chem. Phys.* **2021**, *155*, 154701.

- (64) Botzung, T.; Hagenmüller, D.; Schütz, S.; Dubail, J.; Pupillo, G.; Schachenmayer, J. Dark State Semilocalization of Quantum Emitters in a Cavity. *Phys. Rev. B* **2020**, *102*, 144202.
- (65) Gonzalez-Ballestero, C.; Feist, J.; Gonzalo Badía, E.; Moreno, E.; Garcia-Vidal, F. J. Uncoupled Dark States Can Inherit Polaritonic Properties. *Phys. Rev. Lett.* **2016**, *117*, 156402.
- (66) Purcell, E. M. Spontaneous Emission Probabilities at Radio Frequencies. *Phys. Rev.* **1946**, *69*, 681.
- (67) Kleppner, D. Inhibited Spontaneous Emission. *Phys. Rev. Lett.* 1981, 47, 233–236.
- (68) Satapathy, S.; Khatoniar, M.; Parappuram, D. K.; Liu, B.; John, G.; Feist, J.; Garcia-Vidal, F. J.; Menon, V. M. Selective Isomer Emission via Funneling of Exciton Polaritons. *Sci. Adv.* **2021**, *7*, No. eabi0997.
- (69) Pérez-Sánchez, J. B.; Koner, A.; Stern, N. P.; Yuen-Zhou, J. Simulating Molecular Polaritons in the Collective Regime Using Few-Molecule Models. *Proc. Natl. Acad. Sci. U.S.A.* **2023**, 120, No. e2219223120.
- (70) Coles, D. M.; Somaschi, N.; Michetti, P.; Clark, C.; Lagoudakis, P. G.; Savvidis, P. G.; Lidzey, D. G. Polariton-Mediated Energy Transfer between Organic Dyes in a Strongly Coupled Optical Microcavity. *Nat. Mater.* **2014**, *13*, 712–719.
- (71) Irie, M.; Fukaminato, T.; Matsuda, K.; Kobatake, S. Photochromism of Diarylethene Molecules and Crystals: Memories, Switches, and Actuators. *Chem. Rev.* **2014**, *114*, 12174–12277.
- (72) Kobatake, S.; Hasegawa, H.; Miyamura, K. High-Convertible Photochromism of a Diarylethene Single Crystal Accompanying the Crystal Shape Deformation. *Cryst. Growth Des.* **2011**, *11*, 1223–1229.
- (73) Klajn, R. Spiropyran-Based Dynamic Materials. *Chem. Soc. Rev.* **2014**, *43*, 148–184.
- (74) Feringa, B. L.; Browne, W. R. In *Molecular Switches*; Feringa, B. L., Browne, W. R., Eds.; Wiley-VCH Verlag GmbH & Co. KGaA: Weinheim, Germany, 2011; Vol. 1.
- (75) Stitzel, S.; Byrne, R.; Diamond, D. LED Switching of Spiropyran-Doped Polymer Films. *J. Mater. Sci.* **2006**, *41*, 5841–5844.
- (76) Kortekaas, L.; Browne, W. R. The Evolution of Spiropyran: Fundamentals and Progress of an Extraordinarily Versatile Photochrome. *Chem. Soc. Rev.* **2019**, *48*, 3406–3424.
- (77) Fukaminato, T.; Umemoto, T.; Iwata, Y.; Yokojima, S.; Yoneyama, M.; Nakamura, S.; Irie, M. Photochromism of Diarylethene Single Molecules in Polymer Matrices. *J. Am. Chem. Soc.* **2007**, 129, 5932–5938.
- (78) Guo, H.; Zhang, F.; Wu, G.; Sun, F.; Pu, S.; Mai, X.; Qi, G. Multi-Wavelength Optical Storage of Diarylethene PMMA Film. *Opt. Mater.* **2003**, 22, 269–274.
- (79) Shiraishi, Y.; Inoue, T.; Sumiya, S.; Hirai, T. Entropy-Driven Thermal Isomerization of Spiropyran in Viscous Media. *J. Phys. Chem.* A **2011**, *115*, 9083–9090.
- (80) Sumi, T.; Takagi, Y.; Yagi, A.; Morimoto, M.; Irie, M. Photoirradiation Wavelength Dependence of Cycloreversion Quantum Yields of Diarylethenes. *Chem. Commun.* **2014**, *50*, 3928.
- (81) Thomas, P. A.; Tan, W. J.; Fernandez, H. A.; Barnes, W. L. A New Signature for Strong Light-Matter Coupling Using Spectroscopic Ellipsometry. *Nano Lett.* **2020**, *20*, *6412–6419*.
- (82) Genco, A.; Cruciano, C.; Corti, M.; McGhee, K. E.; Ardini, B.; Sortino, L.; Hüttenhofer, L.; Virgili, T.; Lidzey, D. G.; Maier, S. A.; Bassi, A.; Valentini, G.; Cerullo, G.; Manzoni, C. K -Space Hyperspectral Imaging by a Birefringent Common-Path Interferometer. ACS Photonics 2022, 9, 3563–3572.
- (83) Zhang, Y.; Zhao, M.; Wang, J.; Liu, W.; Wang, B.; Hu, S.; Lu, G.; Chen, A.; Cui, J.; Zhang, W.; Hsu, C. W.; Liu, X.; Shi, L.; Yin, H.; Zi, J. Momentum-Space Imaging Spectroscopy for the Study of Nanophotonic Materials. *Sci. Bull.* **2021**, *66*, 824–838.
- (84) Vasista, A. B.; Sharma, D. K.; Kumar, G. V. P. Fourier Plane Optical Microscopy and Spectroscopy. In *Digital Encyclopedia of Applied Physics*; Wiley-VCH Verlag GmbH & Co. KGaA: Weinheim, Germany, 2019; pp 1–14.
- (85) Shiraishi, Y.; Itoh, M.; Hirai, T. Thermal Isomerization of Spiropyran to Merocyanine in Aqueous Media and Its Application to

- Colorimetric Temperature Indication. Phys. Chem. Chem. Phys. 2010, 12, 13737.
- (86) George, A.; Geraghty, T.; Kelsey, Z.; Mukherjee, S.; Davidova, G.; Kim, W.; Musser, A. J. Controlling the Manifold of Polariton States Through Molecular Disorder. *Adv. Opt. Mater.* **2024**, 2302387.
- (87) Tsubol, Y.; Shimizu, R.; Shoji, T.; Kitamura, N. Near-Infrared Continuous-Wave Light Driving a Two-Photon Photochromic Reaction with the Assistance of Localized Surface Plasmon. *J. Am. Chem. Soc.* **2009**, *131*, 12623–12627.
- (88) Dutta, A.; Tiainen, V.; Duarte, L.; Markesevic, N.; Morozov, D.; Qureshi, H. A.; Groenhof, G.; Toppari, J. J. Ultra-Fast Photochemistry in the Strong Light-Matter Coupling Regime. **2023**, Chemrxiv-2023-6v0hv.
- (89) Agranovich, V. M.; Litinskaia, M.; Lidzey, D. G. Cavity Polaritons in Microcavities Containing Disordered Organic Semiconductors. *Phys. Rev. B* **2003**, *67*, 085311.
- (90) Litinskaya, M.; Reineker, P.; Agranovich, V. M. Fast Polariton Relaxation in Strongly Coupled Organic Microcavities. *J. Lumin.* **2004**, *110*, 364–372.
- (91) Xiang, B.; Ribeiro, R. F.; Chen, L.; Wang, J.; Du, M.; Yuen-Zhou, J.; Xiong, W. State-Selective Polariton to Dark State Relaxation Dynamics. *J. Phys. Chem. A* **2019**, *123*, 5918–5927.
- (92) Xiang, B.; Ribeiro, R. F.; Du, M.; Chen, L.; Yang, Z.; Wang, J.; Yuen-Zhou, J.; Xiong, W. Intermolecular Vibrational Energy Transfer Enabled by Microcavity Strong Light-Matter Coupling. *Science* **2020**, 368, 665–667.
- (93) Schäfer, C.; Flick, J.; Ronca, E.; Narang, P.; Rubio, A. Shining Light on the Microscopic Resonant Mechanism Responsible for Cavity-Mediated Chemical Reactivity. *Nat. Commun.* **2022**, *13*, 7817.
- (94) Wohl, C. J.; Kuciauskas, D. Excited-State Dynamics of Spiropyran-Derived Merocyanine Isomers. *J. Phys. Chem. B* **2005**, 109, 22186–22191.
- (95) Hobley, J.; Pfeifer-Fukumura, U.; Bletz, M.; Asahi, T.; Masuhara, H.; Fukumura, H. Ultrafast Photo-Dynamics of a Reversible Photochromic Spiropyran. *J. Phys. Chem. A* **2002**, *106*, 2265–2270.
- (96) Ruetzel, S.; Diekmann, M.; Nuernberger, P.; Walter, C.; Engels, B.; Brixner, T. Photoisomerization among Ring-Open Merocyanines. I. Reaction Dynamics and Wave-Packet Oscillations Induced by Tunable Femtosecond Pulses. *J. Chem. Phys.* **2014**, *140*, 224310.
- (97) Buback, J.; Nuernberger, P.; Kullmann, M.; Langhojer, F.; Schmidt, R.; Würthner, F.; Brixner, T. Ring-Closure and Isomerization Capabilities of Spiropyran-Derived Merocyanine Isomers. *J. Phys. Chem. A* **2011**, *115*, 3924–3935.
- (98) Amos, R. D.; Kobayashi, R. Ab Initio Investigation of the Structures and Energies of Spiropyran and Merocyanine Isomers. *Mol. Phys.* **2015**, *113*, 1674–1681.
- (99) Cottone, G.; Noto, R.; La Manna, G. Theoretical Study of Spiropyran-Merocyanine Thermal Isomerization. *Chem. Phys. Lett.* **2004**, 388, 218–222.
- (100) Menzonatto, T. G.; Lopes, J. F. The Role of Intramolecular Interactions on the Stability of the Conformers of a Spiropyran Derivative. *Chem. Phys.* **2022**, *562*, 111654.
- (101) Walter, C.; Ruetzel, S.; Diekmann, M.; Nuernberger, P.; Brixner, T.; Engels, B. Photoisomerization among Ring-Open Merocyanines. II. A Computational Study. *J. Chem. Phys.* **2014**, *140*, 224311.
- (102) Pérez-Sánchez, J. B.; Mellini, F.; Giebink, N. C.; Yuen-Zhou, J. Frequency-Dependent Photoreactivity in Disordered Molecular Polaritons. **2023**, arXiv: 2308.03954.